Daytime Sky Brightness Modeling of Haleakala

Kevin T.C. Jim, Brooke Gibson, Edward A. Pier
Oceanit, Oceanit Center, 828 Fort St. Mall, Suite 600, Honolulu, HI 96813

ABSTRACT

We model the brightness of the daytime sky as seen from Haleakala from 0.3 to 5 microns using MODTRAN®5. Our goal was to determine the sky background radiance and transmission as a function of wavelength for imaging applications during the daytime. The sky brightness varies through a modeled day, and this is shown using a set of look angles toward the geosynchronous belt. We compare our results using radiosonde and real weather data recorded at the summit with the default atmospheric model of MODTRAN.

1. INTRODUCTION

Currently, the SSN tracks GEO satellites during the daytime with radar. Radar systems have some limitations, in that they have limited coverage and thus cannot track all satellites. Furthermore, radars are expensive to maintain and operate. An optical telescope system that can monitor satellites during the day would be a useful augmentation to radar tracking. As a less expensive alternative, it could be more widely deployed, and provide additional capabilities for satellite characterization. The most difficult part of optical imaging during the daytime is the bright daytime sky background, and so we have performed some modeling of the sky radiance, coupled with an SNR analysis, to predict the performance of a telescope/camera system.

We are currently building a near infrared camera system which will be mounted to an optical telescope for this purpose. This system is optimized by using the most effective filters and a focal plane array (FPA) sensitive to the optimal passbands as predicted by our modeling.

MODTRAN is the code used to model the atmospheric radiance and transmission. MODTRAN includes six types of geographical-seasonal model atmospheres which can be used, but they are based upon wide-ranging average conditions. A. Berk of Spectral Sciences, one of the authors of MODTRAN, advised us to use the Mid-Latitude Winter model in our initial efforts, but that using radiosonde data would be more accurate [1]. In addition, using actual weather data would improve the accuracy of the models.

To this end, we chose to model the atmospheric radiance and transmission first at the summit of Haleakala on Maui, as it is both well-studied and has operating telescopes that might be employed for daytime imaging. Accurate weather data are required for modeling. The Mees Solar Observatory on Haleakala has weather data dating back to 1994, which we obtained for this modeling effort [2].

2. MODTRAN

The MODerate resolution atmospheric TRANsmission code (MODTRAN) is an advanced radiative transfer simulation of the Earth's atmosphere [3]. It models the atmosphere as thirty layers, each with different physical characteristics. MODTRAN incorporates measured and modeled spectra of all of the dominant molecular and ionic components of the atmosphere, and can model multiple scattering from particles. It is useful from the ultraviolet well into the thermal infrared wavelengths. MODTRAN models the atmosphere to 100 km. MODTRAN is considered a standard code for Air Force atmospheric simulations, and is validated against a large number of test cases. In addition to the six geographical-seasonal model atmospheres included, MODTRAN has the capability to ingest user-specified meteorological data and radiosonde data. The six models are standards consisting of a single-altitude model, Tropical Atmosphere, Mid-Latitude Summer, Mid-Latitude Winter, Sub-Arctic Summer, Sub-Arctic Winter and a 1976 US Standard Atmosphere.

MODTRAN is designed to simulate different geometries and times, and will calculate solar and lunar positions based on those times. Because we were concerned with how the sky brightness would change with time, we needed to model both different look angles and times. While MODTRAN incorporates the ability to do multiple simulations from one input file, in which times and geometries could be changed, we found that it did not work as we intended. As an alternative approach, we separated the set of simulations both in time and in look angles, thus creating a large

number of simulations for a single day. We wrote software to generate the input parameter files for each simulation from tables of values that would vary, using a base input parameter file. Since this is an embarrassingly parallel computation, we wrote a Perl script to distribute these runs on our computing cluster, which consists of eight blade servers, each with 12 cores of 2.4 GHz Intel Xeon processors. By allowing just one job per core at a time, the run time was reduced by 50 times, as compared to a 4-core desktop computer. One simulation day runs in less than 2 hours on the computing cluster.

3. DATA SOURCES AND INPUT TO SIMULATION

3.1 MODTRAN

We simulated two cases: a radiosonde-based simulation and one using the standard Mid-Latitude Winter atmosphere model. This is the model best suited to Haleakala's rarefied and dry conditions; though Haleakala is located in the tropics, the Tropical Atmosphere model is not suited for this location because it is meant for tropical rainforests. The geometry was of an arbitrary slant path, in MODTRAN terminology. The radiance mode was used, and the transmissions were derived from the resultant tape 7 files. The MODTRAN cards (input lines) that were included in the input tape5 file that controls MODTRAN consist of 1, 1A, 2, 2C, 2C1, 3, 3A1, 3A2, 4, and 5. The required CARDS include CARD 1, 1A, 2, 3, 4, and 5, while CARDS 2C and 2C1 were added to include parameters for the user-specified atmosphere.

Two parameter value choices on CARD 1 were used to prompt MODTRAN to read user-specified radiosonde data on CARDS 2C and 2C1. These choices include MODEL = 7 (user-specified model atmosphere) and I_RD2C = 1 to read user input data.

Multiple scattering, spectrally-dependent scattering, and solar azimuthal dependence were selected. We chose to modify the aerosol optical properties as they depend on the changes from the original relative humidity profile which is found from scaling the water column specified by the H2OSTR parameter. To do this, the H2OAER parameter was set equal to T (true). The IHAZE parameter is used to set the aerosol model used. We chose IHAZE = 3 for the NAVY MARITIME extinction. This choice sets the VIS (visibility) parameter by using the wind speed, provided from the empirical weather data, and relative humidity. We used the default water column for the case of the standard atmosphere model, and MODTRAN derived the water column from the radiosonde data in the radiosonde case. The CO_2 concentration was set to 390 ppm, the mean value measured at Mauna Loa in mid-2010 [4]. All other molecular species used the default values for the Mid-Latitude Winter model.

The default band model for solar irradiance (1 cm^{-1} bin size) was used.

3.2 RADIOSONDE

A radiosonde file consists of measurements recorded during a balloon flight including temperature, pressure, geopotential height, dewpoint depression, wind direction, and wind speed. The geopotential height is converted to altitude for input to MODTRAN and dewpoint depression is converted to dewpoint temperature. Radiosonde balloons are released nominally at 00:00 and 12:00 UTC every day from 1500 stations around the world. To assist with simulations of the atmosphere in Hawaii there are a few stations including Lihue, Pu'unene, and Hilo, HI. The Pu'unene station closest to Haleakala has limited data on the dates we were concerned with, so we used data collected at the Hilo station which is the closer of the remaining two to Haleakala.

The data were downloaded from the Integrated Global Radiosonde Archive (IGRA) [5]. The National Climatic Data Center (NCDC) and the NOAA Satellite and Information Service and the National Environmental Satellite, Data, and Information Service (NESDIS) maintain the data set.

3.3 WEATHER DATA

The selection of a day to model entails first choosing a day of year, then locating existing weather data and parsing it to find the year that has the most ideal day chosen. An ideal day is one without rain and with typical visibility and humidity. For example, we chose to model the summer solstice, day 172-173, and a few years of data were parsed in order to find the year during which the summer solstice had good weather. In addition to parsing the data to evaluate the rain, visibility, and humidity, any available imagery was used to get a quick impression of the weather on a par-

ticular day. Imagery in the visible and infrared as well as water vapor imagery are useful for this purpose. Day 172-173 of 2010 turned out to be a day without rain, with visibility typical of the site, and with moderate humidity.

We used the weather data, obtained from the Mees Solar Observatory weather station, shown in Table 2 below. To prepare the weather data as input to MODTRAN certain units were converted. Temperature was converted to Kelvin, visibility to kilometers, and time to decimal time.

Table 1. Descriptions of the weather-related input parameters for MODTRAN [6].

IDAY	Day of the year from 1 to 365 used to specify the earth to Sun distance and (if IPARM = 1) to specify the Sun's location in the sky. (Default value is the mean earth to Sun distance, IDAY = 93).
TIME	Greenwich time in decimal hours, that is, 8:45 a.m. is 8.75, 5:20 p.m. is 17.33 etc. (used with IPARM = 1 or 11).
WSS	Current wind speed (m/s). Used with the Navy Aerosol Maritime (NAM) model (IHAZE = 3) or the DESERT model (IHAZE = 10)
TPTEMP	If the 'area-average' temperature (AATEMP, CARD 4A) is not entered and the line-of-sight intersects the earth, TPTEMP is also used as the lower boundary temperature in the multiple scattering models.
VIS	User specified surface meteorological range (km).
GNDALT	Altitude of surface relative to sea level (km). GNDALT may be negative but may not exceed 6 km. The baseline 0 to 6-km aerosol profiles are compressed (or stretched) based on input GNDALT. GNDALT is set to the first profile altitude when radiosonde data is used (model = 7).
RAINRT	Rain rate
WHH	24-hour average wind speed (m/s). Used with the Navy Aerosol Maritime model (IHAZE = 3).

Table 2. Weather Data from Mees Solar Observatory for Haleakala for the Summer Solstice 2010

IDAY	TIME	WSS	TPTEMP	VIS	GNDALT	RAINRT	WHH
172	15.0	11.5	283.4	50	3	0	5.4
172	16.0	10.6	282.9	50	3	0	5.9
172	17.0	8.3	284.1	50	3	0	6.3
172	18.0	7.2	286.1	50	3	0	6.5
172	19.0	6.5	287.6	50	3	0	6.6
172	20.0	8.0	288.3	50	3	0	6.8
172	21.0	6.9	289.7	49	3	0	7.0
172	22.0	6.9	290.1	50	3	0	7.2
172	23.0	6.1	290.0	50	3	0	7.1
173	0.0	5.2	289.5	50	3	0	7.1
173	1.0	6.5	289.1	50	3	0	7.0
173	2.0	7.8	287.9	50	3	0	7.0
173	3.0	6.7	287.4	49	3	0	7.1
173	4.0	7.2	286.1	50	3	0	7.1
173	5.0	6.5	284.7	50	3	0	7.1
173	6.0	6.4	283.7	50	3	0	7.2

The breadth and quality of weather data at a given site can be a limitation to this method of atmospheric modeling. This was seen when preparations for a user-specified model of the daytime sky brightness at the summit of Mauna Kea were being done. The numerous readily available weather recordings were missing some key data which usually consisted of the measurement of visibility. The Mees Solar Observatory weather station has recorded the most comprehensive weather data we have seen during this process.

3.4 GEO BELT POSITION

A significant difficulty in modeling sky brightness at a fine scale is to determine where to measure the sky brightness. We chose to constrain our efforts to the GEO belt, as observed from Haleakala. The GEO belt position as

viewed from Haleakala was found by downloading the catalog of geosynchronous satellite element sets (elsets) from www.space-track.org. Satellites in this catalog are defined as having a mean motion greater than or equal to 0.99 and less than or equal to 1.01, and an eccentricity less than or equal to 0.01. The satellites were sorted by inclination and the resulting elsets that had an inclination of zero degrees were kept. This remaining list along with the date and time (day 172 at 22:00 UTC) was input to a program called SatView which outputs positional information including azimuth, elevation, range and phase angle of GEO satellites. Only satellite positions having an elevation of 20 degrees or greater were kept in the plot since air masses below that elevation are large. Sixteen satellites survived this filtering. As viewed from Hawaii, the majority of satellites are in the east and in the west with none to represent the higher elevations. A sixth order polynomial was fit to the existing satellite positions so that we could have a representation of the higher elevations and an equation with elevation and range as a function of azimuth. Using this equation, elevations of azimuths at ten degree steps were found and these positions were used as input to MODTRAN.

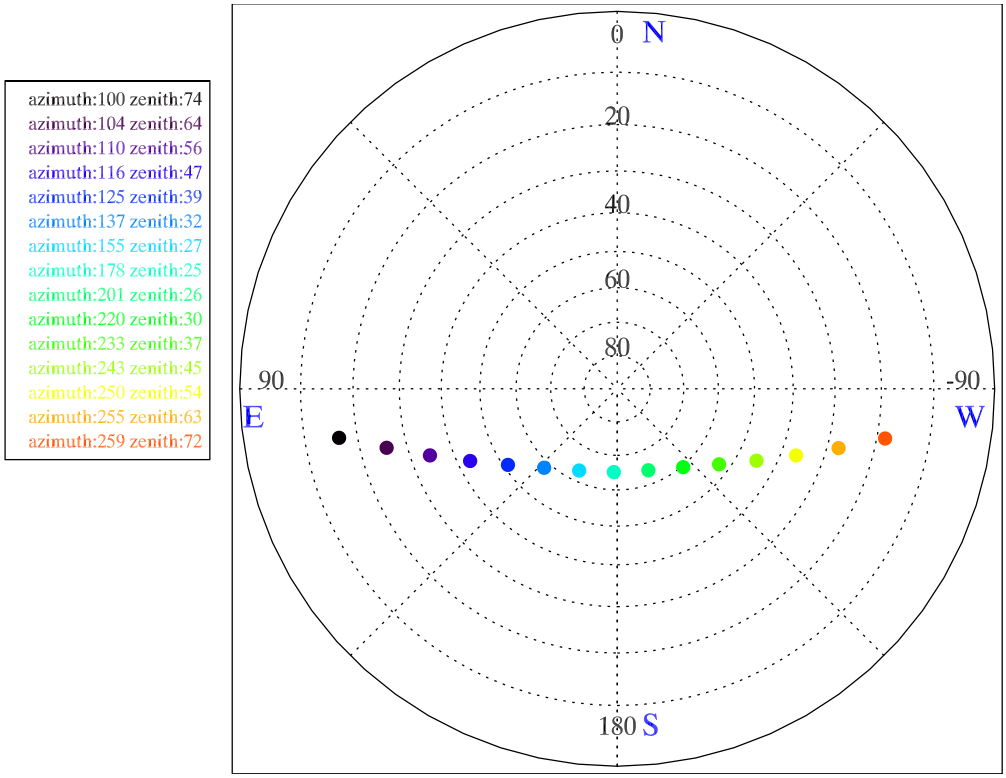

Fig. 1. Positions in altitude and elevation angle of simulated look angles into the GEO belt from Haleakala. Azimuth and zenith angle are shown in the table on the left.

4. RESULTS AND DISCUSSION

In Figs. 2 and 3, the transmittance and radiance of the sky as a function of wavelength and look angle are shown for 6AM local time, just after sunrise. The simulation of Fig. 2 uses the standard Mid-Latitude Winter model, and the one depicted in Fig. 3 uses the radiosonde data from Hilo. At 3 μm, we note that there are features in the standard model case that are not present in the radiosonde-based model. We suspect that the difference comes from the inclusion of higher layers than the radiosonde data, since the radiosonde data has a maximum altitude of 31 km.

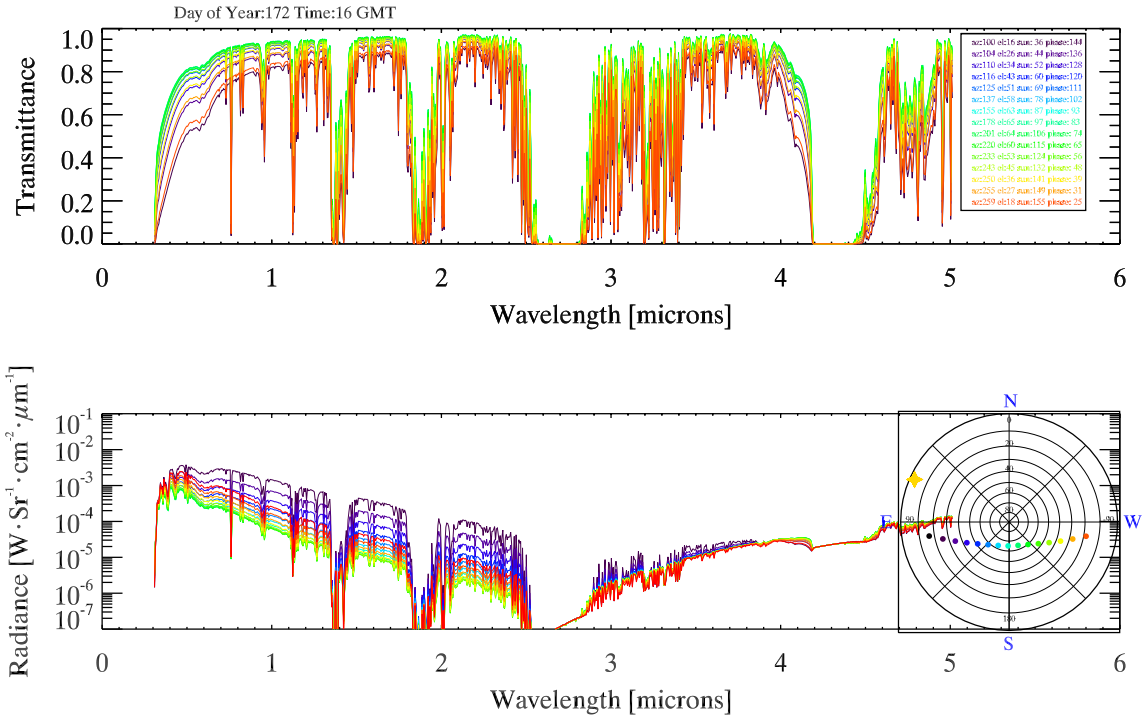

Fig. 2. The transmittance and sky radiance for Haleakala with Mid-Latitude Winter model at 1600 UT = 0600 local time. The look angles are color-coded and their positions are listed in the legend on the top plot and in the diagram on the right on the second plot. The yellow star indicates the sun position.

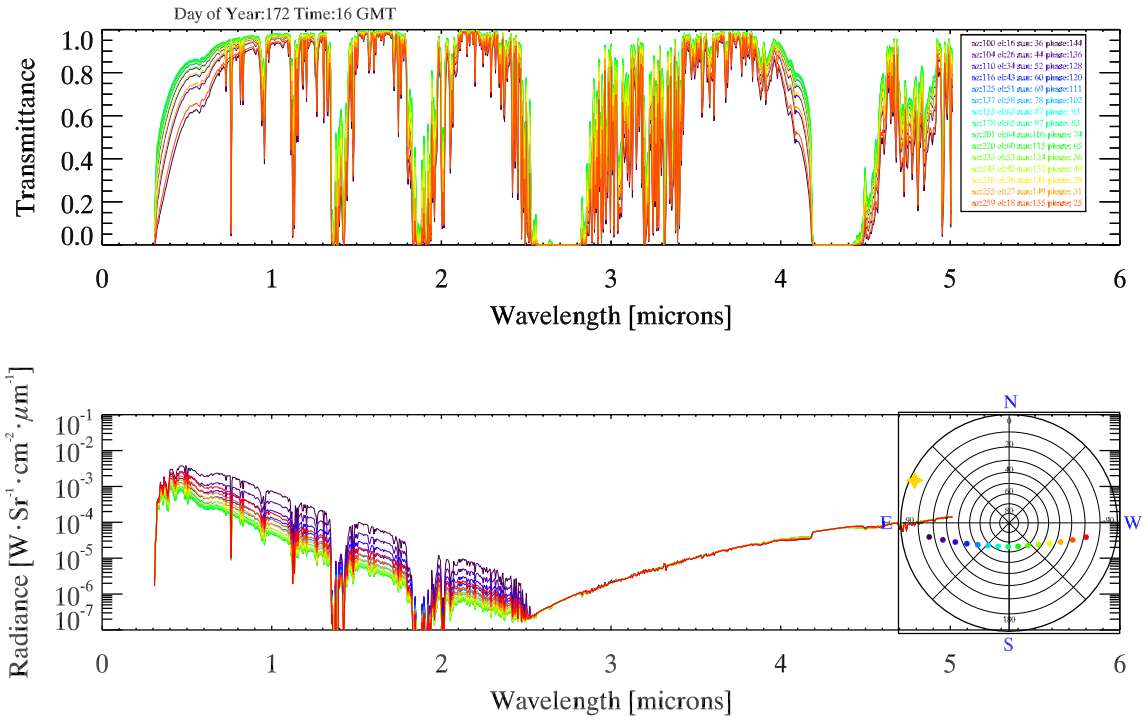

Fig. 3. The transmittance and sky radiance for Haleakala using a radiosonde model are plotted. Note the lack of structure in the radiance plot around 3 μm, unlike the mid-latitude winter model.

Throughout the day, the transmittance does not seem to change much, except in the 0.3 μm to 0.5 μm region, and is largely a function of look angle. The sky radiance, however, changes significantly during the day, becoming brighter closest to noon (Figs. 4 and 5). The difference between different look angles is greatest at lower solar elevations, and there is very little difference in sky brightness at the various look angles at noon.

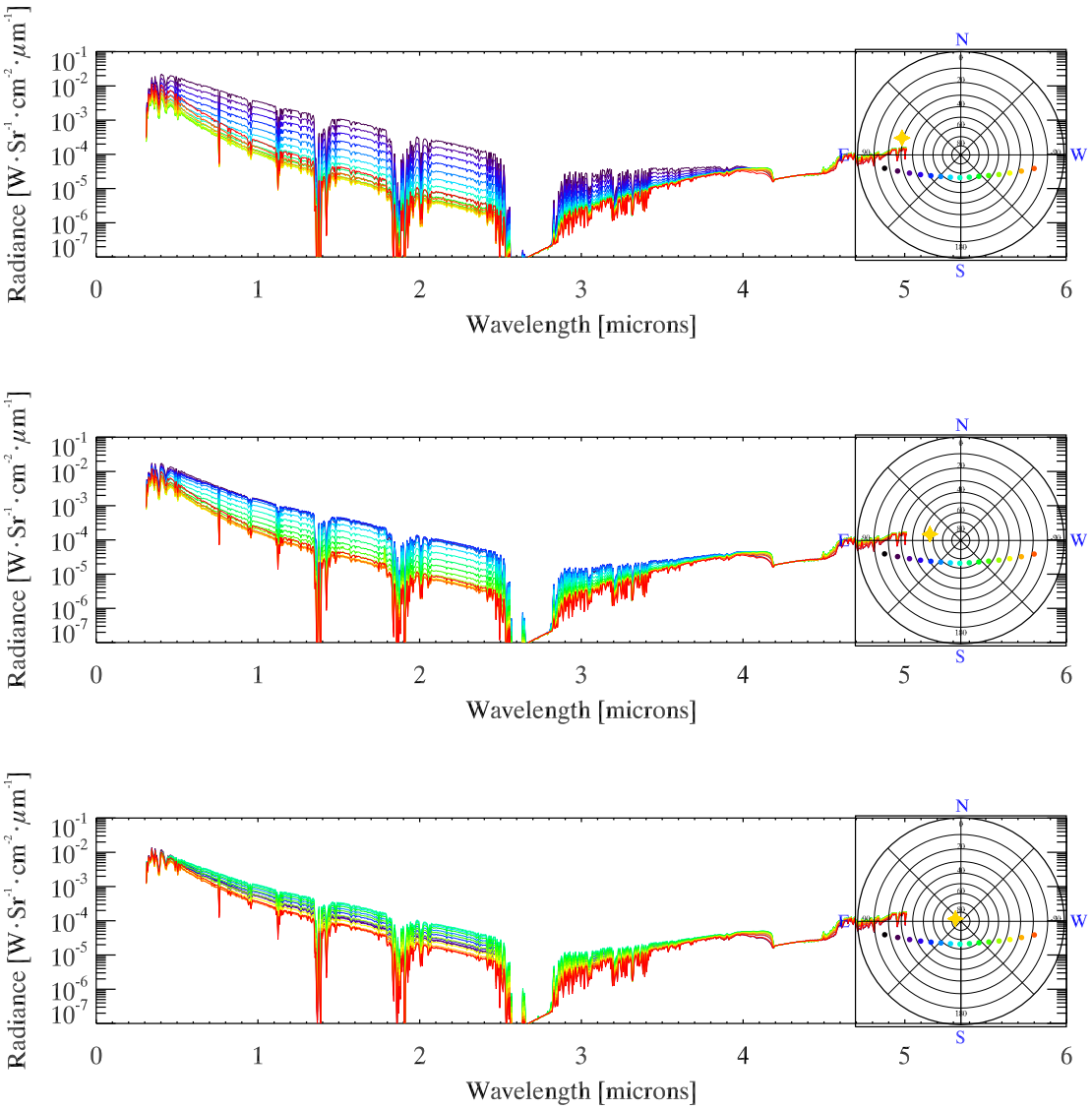

Fig. 4. Sky radiance increases through the morning in the Mid-Latitude Winter model at 8AM, 10AM, and 12PM local time. The sun position is shown in the polar plot.

Comparing Figs. 4 and 5, the sky radiance is greater in the Mid-Latitude Winter model. There also appears to be a greater variation due to look angle in the Mid-Latitude Winter model. In Fig. 6, we have plotted the sky brightness in terms of magnitudes per square arcsecond in the infrared *K* filter (using Vega as the zero-magnitude reference) to show how it varies with time for each model case. The colors of the lines correspond to the look angles as shown in in Figs. 2-5. The sky brightness varies the most for look angles closer to the horizon, but are not symmetric. The bluer lines, which are look angles in the East, are slightly brighter in the afternoon than the Western look angles are in the morning. As the Sun rises, look angles to the far West will brighten briefly more than higher elevation angles (see the redder curves at 7 local time.) The same occurs as the Sun sets for look angles to the far East. The much greater brightness of the Mid-Latitude Winter model is most evident in *K* (Fig. 6) than in *J* or *H*.

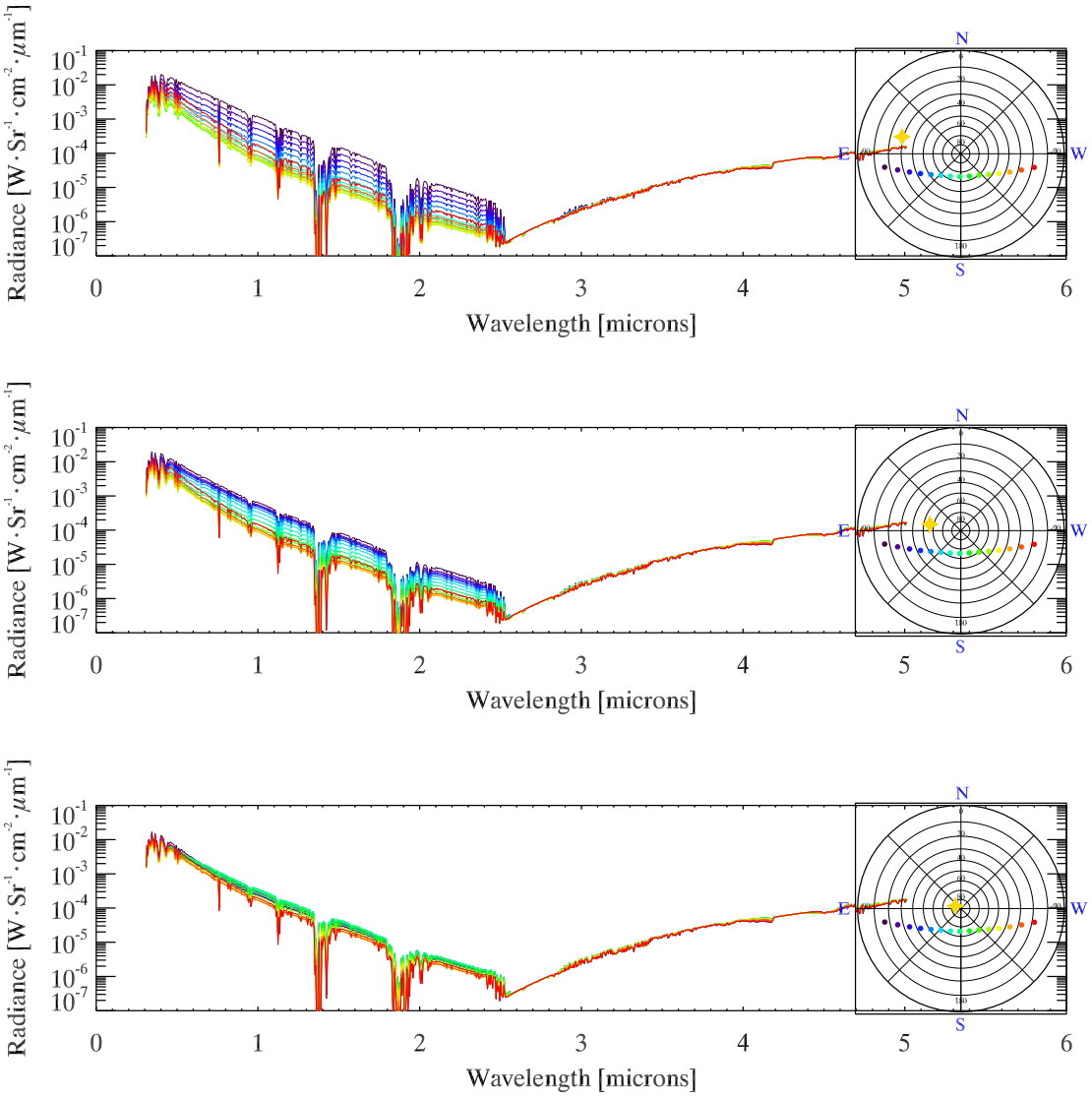

Fig. 5. Sky radiance changes through the morning in this radiosonde-based model, shown at 8AM, 10AM and 12PM local time. Close to noon, the sky brightness is almost the same at all look angles.

Fig. 7 shows the sky brightness as a function of Sun angle, the angle between the Sun and the position in the GEO belt being observed, as seen by the observer. This is the same as the 180° - satellite phase angle. Each line is for a different look angle, and therefore a different air mass. Each dot represents a different time, spaced 1 hour apart, with time generally progressing from left to right. In Fig. 7, all of the look angles are to the East or nearly due South in the highest altitude case.

Except at low air mass near twilight, the sky brightness is a function of two parameters, Sun angle and air mass. The sky is brighter at high air masses because the observer is looking through a higher column of atmosphere. The sky is brightest near the Sun, but dimmest at a Sun angle of around 120 degrees. It becomes brighter again at higher Sun angles due to backscattering. For look angles near the horizon at twilight, the proximity of the horizon introduces more complicated effects.

The difference between the two models is vividly shown in Fig. 8, where for *J* and *K,* we have subtracted the radiosonde model sky brightness from the Mid-Latitude Winter model brightness. We note that at *J*, the Mid-Latitude

Winter model is about 1 magnitude brighter than the radiosonde model, but at *K* the Mid-Latitude Winter model sky brightness is as much as 3.5 magnitudes brighter.

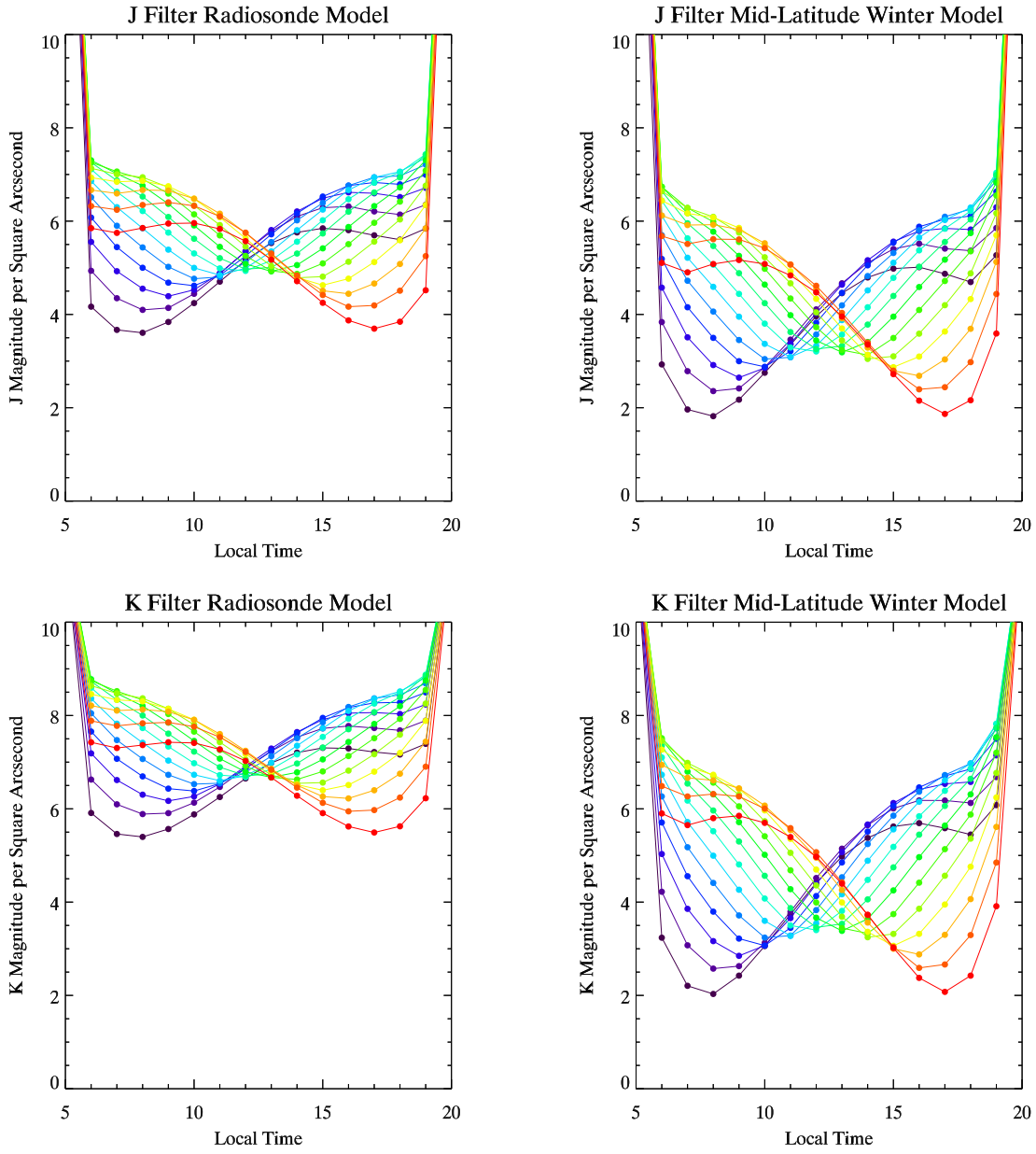

Fig. 6. Sky brightness changes with time for the radiosonde model (left) and the standard Mid-Latitude Winter model (right). The colors correspond to the look angles shown in previous plots. The redder colors in this rainbow color stretch are the more western look angles. The sky brightness is much lower in the radiosonde model. The temporal variations are not completely symmetric, in that the sky is brighter in the afternoon than in the morning.

So which model is closest to reality? The model results need to be compared with actual sky brightness measurements, for which we have some limited data. Informal measurements by J. Rayner at the NASA Infrared Telescope Facility (IRTF) on Mauna Kea [8] show sky brightness between 6 to 6.5 magnitudes per square arcsecond at *J*, *H*, and *K*, at 45° solar angles. This more closely matches the results from the radiosonde model than from the Mid-Latitude Winter model. In the radiosonde model, at 45° solar angles, the sky brightness was between 6 to 7.2 magni-

tudes per square arcsecond in *K,* between 4.9 and ~6.3 in *H,* and between 4.2 and 5.7 in *J*. We are in the process of analyzing other data, but we have not found comparable measurements of daytime sky brightness in the literature.

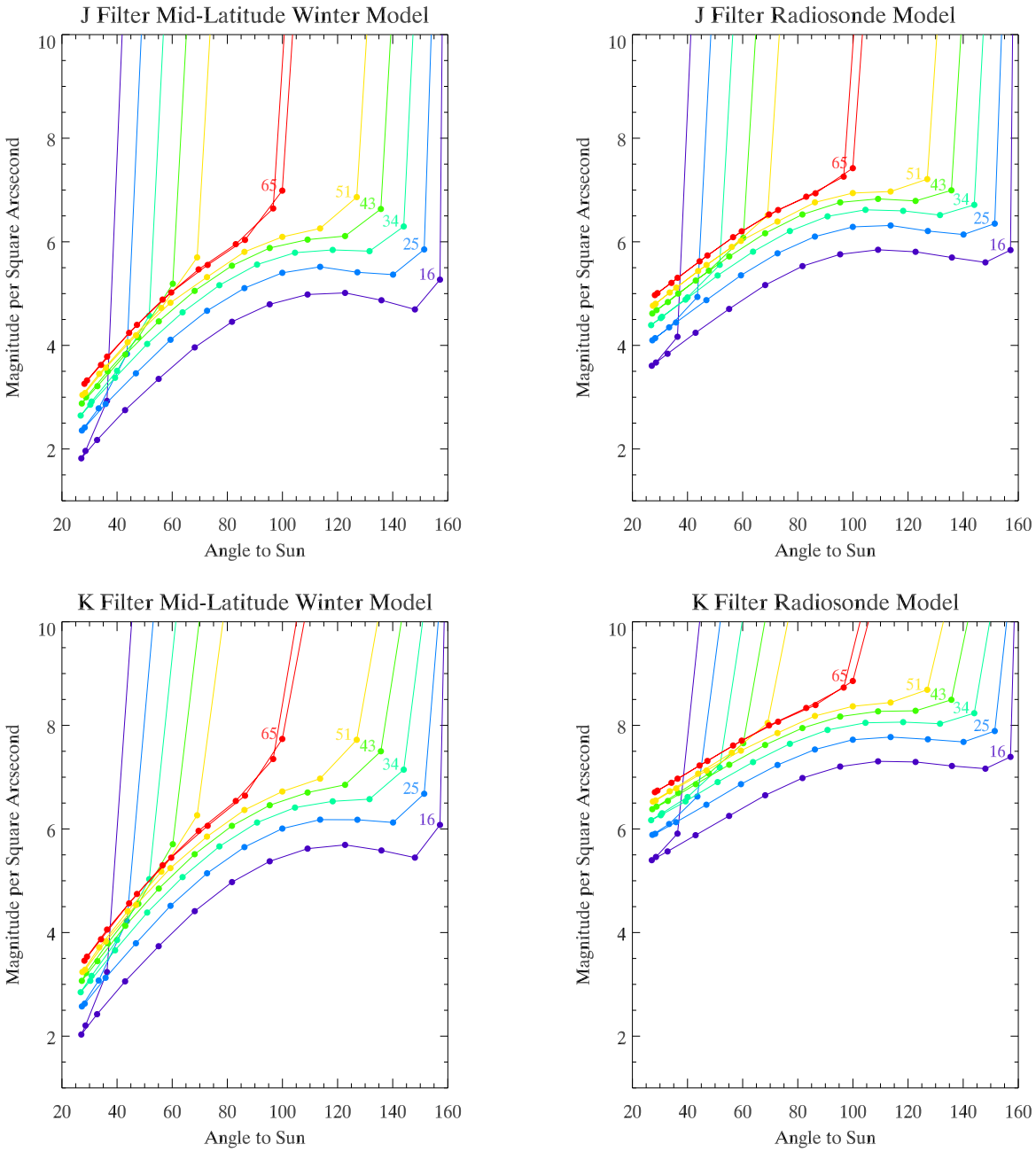

Fig. 7. The sky brightness as a function of angle to the Sun at different altitudes is plotted in magnitudes per square arcsecond. The sky brightness increases with decreasing solar angle, as expected. The colored numbers on the plot indicate the altitude [°] of the selected point in the GEO belt.

5. CONCLUSION AND FUTURE WORK

We have presented the results of MODTRAN-based atmospheric simulations of daytime sky brightness from 0.3 to 5 microns for the particular case of observing the geosynchronous belt from the summit of Haleakala. Fig. 7 summarizes the most useful form of these results. Of the two models considered, the radiosonde-based model produces more accurate results, but that needs to be confirmed more carefully. There may be some problems in the radiosonde

model as we implemented it, and in particular, we note the lack of variation in the sky radiance around 3 μm. We speculate that this may be due to the maximum altitude in the radiosonde model being the altitude at which the radiosonde stops reporting, which is 31 km. While we do not have data above that altitude for the particular location, date, and time of this simulation, we could incorporate the values of higher layers from the Mid-Latitude Winter model into the radiosonde model and compare the results.

In the near future, we will also run simulations for other dates and locations. We have incorporated the results of these atmospheric simulations into code that predicts the SNR of satellite observations, which we are using in the HANDS-IONS project to predict the performance of a system used to observe GEO satellites during the daytime. We will also be gathering more sky brightness observations to validate our model.

This work is sponsored by the Advanced Technology Branch of the Space and Missile Systems Center (AFSPC SMC/SYE) under contract FA8819-10-C-0002, High Accuracy Network Determination System - Intelligent Optical Networks for Space Situational Awareness (HANDS-IONS), with Program Manager Capt. Eric Charest. The authors gratefully acknowledge the insight and advice of Dr. Donald Davies and Dr. Ray Russell of the Aerospace Corporation and of Dr. Earl Spillar of AFRL.

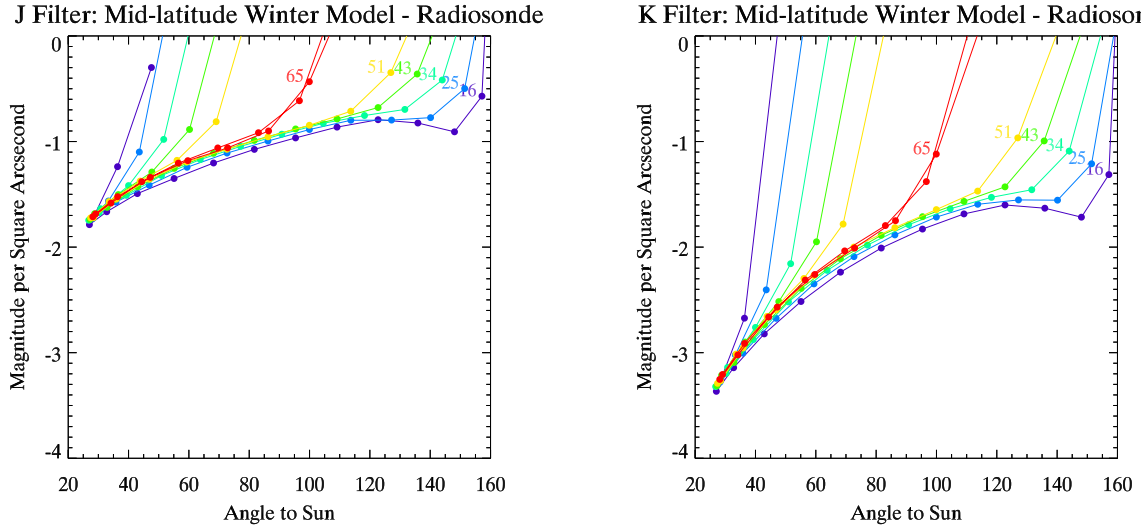

Fig. 8. The Radiosonde model sky brightness is subtracted from the Mid-Latitude Winter model brightness for *J* and *K*, showing that the Radiosonde model is fainter.

6. REFERENCES

1. Berk, A., Spectral Sciences, private communication. 2010.
2. Kuhn, J., Institute for Astronomy, University of Hawaii, private communication, 2010.
3. Berk, A., Anderson, G. P., Bernstein, L. S., Acharya, P. K., Dothe, H., Matthew, M. W., Adler-Golden, S. M., Chetwynd, J. H., Richtsmeier, S. C., Pukall, Brian, Allred, Clark L., Jeong, L. S., Hoke, and Michael L., MODTRAN4 Radiative Transfer Modeling for Atmospheric Correction, Proc. SPIE, Vol. 3756, p. 348-353, Optical Spectroscopic Techniques and Instrumentation for Atmospheric and Space Research III, Allen M. Larar; Ed., 1999.
4. C.D. Keeling, R.B. Bacastow, A.E. Bainbridge, C.A. Ekdahl, P.R. Guenther, and L.S. Waterman, Atmospheric carbon dioxide variations at Mauna Loa Observatory, Hawaii, Tellus, Vol. 28, 538-551, 1976. Data available at http://www.esrl.noaa.gov/gmd/ccgg/trends/
5. Integrated Global Radiosonde Archive, 2011, http://www.ncdc.noaa.gov/oa/climate/igra/
6. Berk, A., Anderson, G.P., Acharya, P.K., Shettle, E.P., MODTRAN 5.2.0.0 User's Manual, Spectral Sciences, Inc., Burlington, MA and AFRL, Space Vehicles Directorate, Hanscom AFB, MA, 2008.
7. Rayner, J., NASA IRTF, Institute for Astronomy, University of Hawaii, private communication, 2010.